

EA-KD: Entropy-based Adaptive Knowledge Distillation

Chi-Ping Su^{1,*}, Ching-Hsun Tseng^{2,*}, Bin Pu³, Lei Zhao⁴, Zhuangzhuang Chen³, Shin-Jye Lee^{1,†}

¹National Yang Ming Chiao Tung University, ²The University of Manchester,

³Hong Kong University of Science and Technology, ⁴Hunan University

Abstract

Knowledge distillation (KD) enables a smaller “student” model to mimic a larger “teacher” model by transferring knowledge from the teacher’s output or features. However, most KD methods treat all samples uniformly, overlooking the varying learning value of each sample and thereby limiting effectiveness. In this paper, we propose Entropy-based Adaptive Knowledge Distillation (EA-KD), a simple yet effective plug-and-play KD method that prioritizes learning from valuable samples. EA-KD quantifies each sample’s learning value by strategically combining the entropy of the teacher and student output, then dynamically reweights the distillation loss to place greater emphasis on high-value samples. Extensive experiments across diverse KD frameworks and tasks—including image classification, object detection, and large language model (LLM) distillation—demonstrate that EA-KD consistently enhances performance, achieving state-of-the-art results with negligible computational cost. Our code will be publicly available.

1. Introduction

The increasing size of state-of-the-art (SOTA) deep learning models in computer vision (CV) [6, 21, 32], and large language models (LLMs) [5, 25] pose challenges for deployment in resource-constrained settings. Knowledge Distillation (KD) [9] offers a solution by training a smaller “student” model to mimic a larger “teacher” model, using both ground-truth labels and the teacher’s “knowledge” (e.g. softened logits or feature representations) to achieve similar performance in a compact form.

SOTA KD methods have explored diverse knowledge forms and structural modifications to refine knowledge transfer [1, 9, 11, 19, 24, 26, 38]. However, most methods distill uniformly across all samples, operating under the assumption that each sample has equal importance and overlooking their varying learning needs. Recent advancements, such as Instance-T [16], have shown that assigning unique temperatures to each sample outperforms the uniform tem-

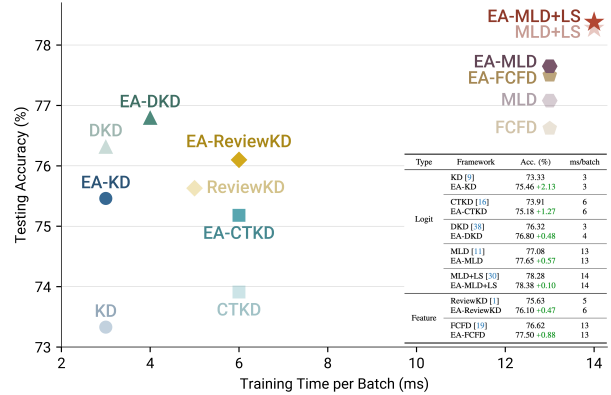


Figure 1. Training Time per Batch (ms) vs. Testing Accuracy (%) on CIFAR-100. Highlighting EA methods’ enhanced performance with minimal additional training cost.

perature method Global-T. This highlighted the benefits of adapting to each sample’s distinct characteristics. Building on this, we hypothesize that emphasizing samples rich in *valuable knowledge*¹ can further optimize the distillation process. This mimics how human students learn better when key points are highlighted by teachers, and thus, this targeted approach allows the student model to achieve better comprehension by focusing on more informative samples. As we will demonstrate, the uniform distillation in most KD methods also tends to overshadow these important samples, limiting the efficiency of knowledge transfer.

The question then arises: *How can we identify the most valuable samples for learning?* Entropy, the core concept in information theory that quantifies the uncertainty or information of a random variable [28], may be well-suited for this role. While a prior multi-teacher KD study utilized inverse entropy to measure the reliability of teachers’ output [13], this method does not apply to the more prevalent single-teacher setting. Moreover, relying solely on the teacher’s entropy restricts the adaptability to the evolving learning dynamics of the student, leaving the full potential of entropy in KD under-explored. Therefore, we propose leveraging entropy to quantify the learning value of each

*Equal contribution

†Corresponding author: camhero@gmail.com

¹Throughout this paper, we consider samples with high entropy as containing valuable knowledge.

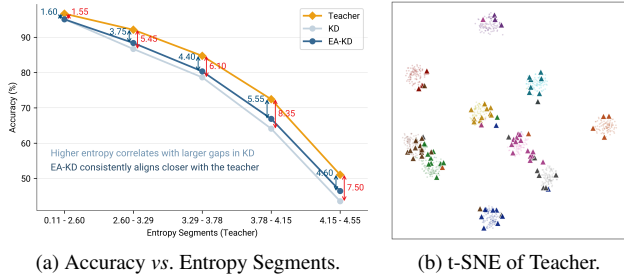


Figure 2. **High-Entropy Samples in KD.** (a) Higher teacher entropy correlates with larger accuracy gaps in KD, while EA-KD maintains closer alignment. (b) The top 10% of high entropy samples (denoted by triangles) cluster near decision boundaries, representing critical knowledge essential for classification.

Table 1. **Entropy-based Reweighting on KD.** Reweighting with entropy (H^T and H^S) improves student’s performance, while inverted reweighting ($H_{ub} - w$) reduces accuracy.

Loss Function	Reweighting Factor w	
	H^T	H^S
L_{KD} [9]	73.33	
wL_{KD}	75.14 +1.81	74.76 +1.43
$(H_{ub} - w)L_{KD}$	72.73 -0.60	68.90 -4.43

sample in KD, as high-entropy outputs shall correspond to greater information contents that are crucial for learning. Our preliminary analysis reveals that higher entropy samples² (i) correlate with larger teacher-student accuracy gaps (Fig. 2a) and (ii) often lie near class boundaries in t-SNE visualizations [33] (Fig. 2b), suggesting these informative samples not only offer valuable learning opportunities but are also pivotal in defining decision boundaries. Hence, entropy can serve as a reliable metric for identifying valuable samples that are crucial for learning in KD.

Leveraging this insight, adapting the focus of KD to valuable samples through entropy reweighting should fill the need for enhanced distillation. We conducted a preliminary experiment that compared the performance of reweighting with teacher (H^T) and student (H^S) entropy, along with their linear-inverted variants ($H_{ub} - w$), where high-entropy samples received lower weight. Here, H_{ub} is the upper bound of entropy (\log_{10} for CIFAR-100). As shown in Tab. 1, reweighting with either H^T or H^S significantly improved KD accuracy, while inverted reweighting led to decreased performance. This supports our hypothesis that focusing on samples with valuable knowledge enhances student learning, with H^T proving more effective due to the teacher’s more reliable assessment of sample value.

Exploring deeper, we observed that H^S exhibited increasing variability across training epochs for the top 10%

²Results for high teacher entropy samples are shown here; high student entropy plots are in the Appendix A.1.

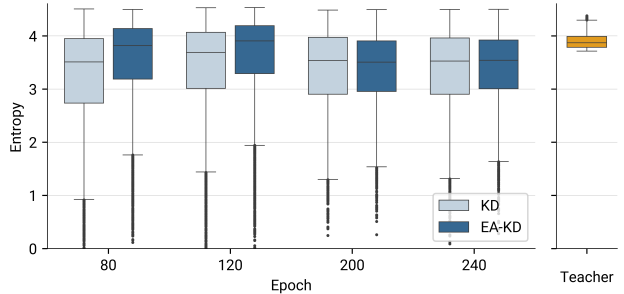


Figure 3. **Box Plot of Student vs. Teacher Entropy for Top 10% High Entropy Samples Across Epochs.** H^S shows significant variations for high H^T samples, highlighting the student’s different views from the teacher. EA-KD achieves improved mimicry of the teacher with more stable entropy and better alignment.

H^T samples (Fig. 3). This suggests that while the teacher finds these samples valuable, potentially due to the inherent differences in architecture or capacity, the student’s assessment fluctuates during training. Some samples remain consistently challenging (high H^S), while others become progressively simpler (low H^S) over time. This misalignment reveals the limitation of reweighting solely with H^T , as it remains constant throughout the epochs and thus fails to capture the student’s evolving learning process.

In light of the above analysis, we introduce Entropy-based Adaptive Knowledge Distillation (EA-KD), a simple yet effective plug-and-play KD method that directs learning toward high-value samples by reweighting the distillation loss. Leveraging both teacher and student entropies, EA-KD emphasizes samples that encapsulate critical knowledge as identified by the teacher, while dynamically adapting to the student’s evolving needs. Intuitively, this method addresses a fundamental limitation in standard KD frameworks, which often overlook the unique learning value of each sample and tend to bias towards simpler knowledge ones. Furthermore, EA-KD can be seamlessly integrated into most KD frameworks, enhancing their performance with negligible computational cost (Fig. 1). Extensive experiments on image classification, object detection, and LLM distillation demonstrate its efficacy and versatility across diverse KD frameworks. Our main contributions are summarized as follows.

- We propose EA-KD, a plug-and-play KD method that adaptively reweights the distillation loss to prioritize samples valuable for learning, enabling a more nuanced and efficient knowledge transfer process.
- We show that high-entropy samples carry critical knowledge in KD, and propose an entropy-based reweighting factor that integrates both teacher and student entropy for a tailored and dynamic focus on these samples.
- We show that EA-KD consistently enhances performance in both logit- and feature-based KD across CV and LLM tasks, achieving SOTA results with negligible cost.

2. Related Work

Logit and Feature Distillation. Logit distillation [9, 11, 38] aligns the softened output logits of the teacher and student, valued for its simplicity and broad applicability. On the other hand, feature distillation minimizes divergence in intermediate feature representations, offering enhanced learning but often with higher computational costs [1, 19, 26]. Both pathways have achieved SOTA performance across tasks and domains. However, most of them typically adopt a static distillation scheme, such as treating all samples uniformly. Adaptive distillation addresses this limitation by introducing more dynamic knowledge transfer processes [13, 16, 20, 22, 30].

Adaptive Distillation. These methods refine knowledge transfer by adapting to data characteristics, student capabilities, or training dynamics. For instance, LS [30] uses Z-score standardization on logits, allowing the student to focus on essential relationships in the teacher’s output. CTKD [16] and MKD [20] adjust the temperature parameter to meet student needs, with Instance-T [16] highlighting the effectiveness of sample-wise adjustments. RW-KD [22] improves distillation by using meta-learning to find optimal weights for each sample. However, these methods often increase complexity and computational costs [16, 20, 22] or are limited to a specific type of KD [30]. In contrast, EA-KD offers a straightforward, more interpretable approach that is versatile across diverse KD frameworks.

Entropy in KD. Previous work introduced an entropy-based metric to quantify knowledge in KD, measuring how much visual information is retained or discarded [2]. Inspired by this, we adopted the entropy of model output to identify valuable samples in KD. AKD [13], which also leverages entropy in KD, adjusts weights based on teacher entropy in multi-teacher distillation, placing greater emphasis on low-entropy predictions. On the contrary, our approach prioritizes high-entropy samples in single-teacher distillation. While low entropy may indicate reliable knowledge in multi-teacher schemes, we view lower entropy as simpler knowledge and is less beneficial for student learning in a single-teacher context, as demonstrated in our preliminary analysis and experiments in Sec. 1.

3. Methodology

3.1. Preliminaries

Information Theory. Entropy quantifies the uncertainty or information content of a random variable [28]. For a given sample x_n , the entropy H_n is computed as follows:

$$H_n = - \sum_{j=1}^C \sigma(z_{n,j}) \log(\sigma(z_{n,j})), \quad (1)$$

where $\sigma(\cdot)$ denotes the softmax function, $z_{n,j}$ is the logit for class j of sample x_n , and C is the number of classes.

Knowledge Distillation. The goal of vanilla KD is to transfer the knowledge encapsulated in the teacher’s softened probability outputs to the student [9]. In classification tasks, the probabilities p are softened using the temperature-scaled softmax function:

$$p_i(T) = \sigma(z, T)_i = \frac{\exp(\frac{z_i}{T})}{\sum_{j=1}^C \exp(\frac{z_j}{T})}, \quad (2)$$

where $p_i(T)$ denotes the softened probability for class i , and $\sigma(z_i, T)$ is the temperature-scaled softmax function. The temperature T controls the smoothness of the distribution, revealing the subtle inter-class relationships.

The core of KD is to minimize the Kullback-Leibler divergence (KLD) between the teacher’s and student’s softened probabilities, the KD loss is defined as:

$$\begin{aligned} L_{\text{KD}} &= \text{KL}(p^{\mathcal{T}}(T) \| p^{\mathcal{S}}(T)) \cdot T^2 \\ &= \sum_{j=1}^C p_j^{\mathcal{T}}(T) \log \left(\frac{p_j^{\mathcal{T}}(T)}{p_j^{\mathcal{S}}(T)} \right) \cdot T^2, \end{aligned} \quad (3)$$

where $p^{\mathcal{T}}$ and $p^{\mathcal{S}}$ denote the teacher’s and student’s softened outputs, respectively. For simplicity of theoretical analysis, we set $T = 1$ in this section. L_{KD} then simplifies to:

$$L_{\text{KD}} = \sum_{j=1}^C p_j^{\mathcal{T}} \log \left(\frac{p_j^{\mathcal{T}}}{p_j^{\mathcal{S}}} \right). \quad (4)$$

3.2. EA-KD

Limitations in Standard KDs. Most logit- and feature-based KD methods typically apply a uniform distillation across all samples, overlooking their unique learning value. This oversight can cause the model to over-prioritize simpler samples at the expense of more valuable, high-entropy ones. Taking KLD—the main loss function for logit-based methods—as an example, consider a student initialized with a uniform distribution $p^{\mathcal{S}}$ where $p_i^{\mathcal{S}} = \frac{1}{C} \forall i$. For a low-entropy sample with a teacher output $p_{\text{low}}^{\mathcal{T}}$ where $p_{\text{low},j}^{\mathcal{T}} \approx 1$ and $p_{\text{low},i}^{\mathcal{T}} \approx 0$ ($i \neq j$), the KLD simplifies to:

$$\begin{aligned} \text{KL}(p_{\text{low}}^{\mathcal{T}} \| p^{\mathcal{S}}) &\approx p_{\text{low},j}^{\mathcal{T}} \cdot \log \left(\frac{p_{\text{low},j}^{\mathcal{T}}}{p_j^{\mathcal{S}}} \right) \\ &= \log \left(\frac{1}{p_j^{\mathcal{S}}} \right) \\ &= \log(C). \end{aligned} \quad (5)$$

For a high-entropy distribution $p_{\text{high}}^{\mathcal{T}} \approx \frac{1}{C} \forall i$, the KLD is:

$$\begin{aligned} \text{KLD}(p_{\text{high}}^{\mathcal{T}} \| p^{\mathcal{S}}) &\approx \sum_{j=1}^C \frac{1}{C} \cdot \log \left(\frac{1/C}{1/C} \right) \\ &= 0. \end{aligned} \quad (6)$$

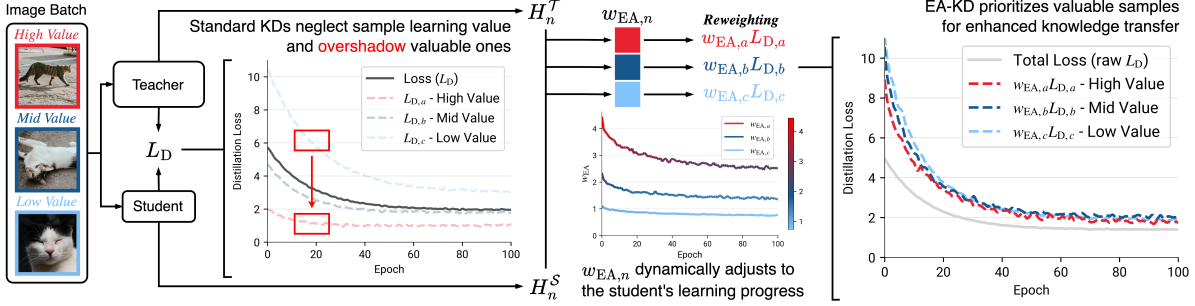


Figure 4. **Illustration of the Uniform Distillation Scheme in Standard KD (Left) and Entropy-based Adaptive Reweighting in EA-KD (Right).** The uniform distillation scheme overlooks the learning value of individual samples, while EA-KD prioritizes valuable samples based on both teacher and student assessments.

Thus, we obtain:

$$\text{KLD}(p_{\text{low}}^T \| p^S) > \text{KLD}(p_{\text{high}}^T \| p^S). \quad (7)$$

This inequality highlights KLD’s overemphasis on low-entropy samples, causing them to dominate the loss over high-entropy ones. Similarly, MSE loss in feature-based methods also biases learning toward high-magnitude activations, which typically correspond to low-entropy samples. Such imbalance shifts the learning focus toward simpler samples, hindering the transfer of knowledge crucial for learning, especially during early training stages (refer to the overshadowing effect in the left part of Fig. 4).

Entropy-Based Reweighting. As discussed in Sec. 1, entropy can serve as a measure of the sample learning value in KD. In practice, we soften the entropy with an alternative temperature T' to better capture the value, expressed as:

$$H_n = - \sum_{j=1}^C p_{n,j}(T') \log(p_{n,j}(T')), \quad (8)$$

where $p_{n,j}(T')$ is the temperature-scaled probability of class j for sample x_n .

To effectively target and emphasize samples valuable for the student, EA-KD’s reweighting factor w_{EA} is formulated using two components: a base term w_{base} and an interaction term w_{interact} . The base term captures the inherent value of each sample based on the teacher’s output entropy, defined as:

$$w_{\text{base},n} = H_n^T, \quad H_n^T \in [0, H_{\text{ub}}], \quad (9)$$

where H_n^T is the entropy of the teacher’s prediction for sample x_n , and $H_{\text{ub}} = \log(C)$ denotes the upper bound of entropy for C classes. The interaction term w_{interact} , on the other hand, captures the interplay between the teacher and student perspectives by taking the normalized product of their entropies:

$$w_{\text{interact},n} = \frac{H_n^T \cdot H_n^S}{H_{\text{ub}}}, \quad w_{\text{interact},n} \in [0, H_{\text{ub}}]. \quad (10)$$

where H_n^S is the student’s entropy. Finally, the EA-KD reweighting factor $w_{EA,n}$ is defined as the average of the base and interaction terms:

$$w_{EA,n} = \frac{w_{\text{base},n} + w_{\text{interact},n}}{2}, \quad w_{EA,n} \in [0, H_{\text{ub}}]. \quad (11)$$

By integrating both the teacher’s evaluation and the student’s evolving understanding, w_{EA} effectively prioritizes valuable samples while dynamically adjusting the focus throughout training.

Reformulation. To better illustrate the influence of the student’s perspective in $w_{EA,n}$, we reformulate Eq. (11) as:

$$\begin{aligned} w_{EA,n} &= \frac{H_n^T + \frac{H_n^T \cdot H_n^S}{H_{\text{ub}}}}{2} \\ &= \frac{1}{2} H_n^T \left(1 + \frac{H_n^S}{H_{\text{ub}}} \right). \end{aligned} \quad (12)$$

This reformulation expresses $w_{EA,n}$ as a product of the H_n^T and a scaling factor that depends on the H_n^S/H_{ub} . In this way, the teacher’s assessment of sample value is adaptively adjusted based on the student’s perspective. Depending on the entropy values, w_{EA} behaves as follows:

$$w_{EA,n} = \begin{cases} H_{\text{ub}} & \text{if } H_n^T \rightarrow H_{\text{ub}} \wedge H_n^S \rightarrow H_{\text{ub}} & (13a) \\ \frac{H_{\text{ub}}}{2} & \text{if } H_n^T \rightarrow H_{\text{ub}} \wedge H_n^S \rightarrow 0 & (13b) \\ 0 & \text{if } H_n^T \rightarrow 0 \quad \forall H_n^S & (13c) \\ w_{EA,n} & \text{otherwise.} \end{cases}$$

When the teacher considers a sample highly valuable for learning ($H_n^T \rightarrow H_{\text{ub}}$), the scaling factor adjusts $w_{EA,n}$ based on the student’s view. If the student aligns (Eq. (13a)), the weight is maximized to emphasize this sample. Conversely, if the student is confident (Eq. (13b)), the weight reduces to half for moderate focus. However, when the teacher considers the sample simple (Eq. (13c)), the weight remains low regardless of H_n^S , as the teacher considers it lacks valuable knowledge.

Table 2. **Results on CIFAR-100.** Accuracy (%) of EA-methods vs. originals across teacher-student pairs, with relative improvements highlighted. Avg. Δ shows average improvement across methods and model pairs. Best results are **bolded**, and second-best are underlined.

Type	Teacher	ResNet32×4	WRN-28-4	WRN-40-2	VGG13	VGG13	ResNet50	ResNet32×4	Avg. Δ
	Student	ResNet8×4	WRN-16-2	WRN-40-1	VGG8	MN-V2	MN-V2	SN-V2	
Logit	KD [9]	73.33	75.04	73.54	72.98	67.37	67.35	74.45	
	EA-KD	75.46 +2.13	75.79 +0.75	74.38 +0.84	74.08 +1.10	69.17 +1.80	69.67 +2.32	75.91 +1.46	+1.48
	CTKD [16]	73.91	75.29	73.93	73.52	68.46	68.47	75.31	
	EA-CTKD	75.18 +1.27	75.72 +0.43	74.03 +0.10	73.79 +0.27	69.19 +0.73	69.38 +0.91	76.02 +0.71	+0.63
	DKD [38]	76.32	76.45	74.81	74.68	69.71	70.35	77.07	
	EA-DKD	76.80 +0.48	76.74 +0.29	74.98 +0.17	75.07 +0.39	70.39 +0.68	70.98 +0.63	77.72 +0.65	+0.47
	MLD [11]	77.08	76.83	75.35	75.18	70.57	71.04	78.44	
	EA-MLD	77.65 +0.57	<u>77.47</u> +0.64	<u>75.77</u> +0.42	75.28 +0.10	70.72 +0.15	<u>71.43</u> +0.39	<u>78.85</u> +0.41	+0.38
	MLD+LS [30]	78.28	77.20	75.56	75.22	<u>70.94</u>	71.19	78.76	
	EA-MLD+LS	78.38 +0.09	77.60 +0.39	75.78 +0.22	75.38 +0.16	70.67 -0.27	71.36 +0.17	79.13 +0.37	+0.16
	ReviewKD [1]	75.63	76.39	74.45	74.45	70.37	69.89	77.78	
	EA-ReviewKD	76.10 +0.47	76.95 +0.56	75.43 +0.98	74.56 +0.11	70.55 +0.18	69.80 -0.09	78.22 +0.44	+0.38
Feature	FCFD [19]	76.62	77.00	75.46	75.22	70.65	71.00	78.18	
	EA-FCFD	77.50 +0.88	77.15 +0.15	75.30 -0.16	<u>75.36</u> +0.14	71.02 +0.37	71.97 +0.97	78.75 +0.56	+0.42
	Avg. Δ	+0.84	+0.46	+0.37	+0.33	+0.52	+0.76	+0.66	+0.56

Loss Integration. As shown in Fig. 4, the flexible nature of w_{EA} allows it to be plug-and-play into most distillation frameworks by reweighting the contribution of each sample based on its learning value. For instance, when integrated with vanilla KD, the loss is defined as:

$$\begin{aligned}
 L_{EA-KD} &= \sum_{n=1}^N w_{EA,n} \cdot L_{KD,n} \\
 &= \sum_{n=1}^N w_{EA,n} \cdot \text{KL}(p_n^T \| p_n^S),
 \end{aligned}
 \tag{14}$$

where $L_{KD,n}$ is the distillation loss for sample x_n , and p_n^T and p_n^S denote the teacher and student’s softened probability for x_n , respectively. Consequently, EA-KD introduces a more nuanced and dynamic knowledge transfer to standard KD frameworks, ensuring that valuable samples receive enhanced focus throughout training.

4. Experiments

4.1. Experimental Setup

Datasets. We used CIFAR-100 [12] (50k training, 10k validation images; 100 classes) and Tiny-ImageNet [14] (100k training, 5k validation images; 200 classes) to evaluate our method for image classification, and used MS-COCO [18] (118k training, 5k validation images; 80 classes) for object detection. Furthermore, for LLM distillation, we employed five instruction-following datasets following [7]: Dolly [4], SInst [34], Vicuna [3], S-NI [35], and UnNI [10].

KD Frameworks. We evaluated EA-KD across representative SOTA logit-based (KD [9], CTKD [16], DKD [38],

MLD [11], MLD+LS [30]) and feature-based methods (ReviewKD [1], FCFD [19]), reweighting their distillation loss while preserving each framework’s original structure. For fair comparisons, no hyperparameter was tuned for the EA-variants, except for the KD weight of MLD+LS [30] was reduced from 9.0 to 4.0 to avoid over-penalizing.

Implementation Details. The EA-KD and other variants were evaluated on various CNNs (VGG [29], ResNet [8], WideResNet [36], MobileNet [27], ShuffleNet [23]), vision transformer teachers (ViT [6], DeiT [32], Swin [21]), and GPT2 [25] for LLM distillation. We used the training settings of [31] for vanilla KD and the respective settings of each KD framework for CIFAR-100 and Tiny-ImageNet, [1] for MS-COCO, and [37] for LLMs. We set $T' = 3$ based on our ablation study, except $T' = 2$ for transformer teachers. All results averaged over five runs, and analyses were conducted using a ResNet32×4 teacher and a ResNet8×4 student on CIFAR-100.

4.2. Results

CIFAR-100. Tab. 2 presents results of various EA-methods and their baselines on CIFAR-100. EA-KD consistently improves both logit- and feature-based KD frameworks across most teacher-student pairs, with an average gain of 0.56%. The logit-based EA-MLD+LS achieved SOTA results in most pairings, while EA-FCFD excelled in two heterogeneous pairs. Additionally, EA-MLD and EA-FCFD secured most second-best results, outperforming the previous SOTA, MLD+LS [30]. These findings highlight EA-KD’s broad applicability and effectiveness in enhancing knowledge transfer across diverse types of KD frameworks.

Table 3. **Results on Tiny-ImageNet.** Top-1 (first row) and top-5 accuracy (second row) for both EA-methods and their original versions using ResNet32×4 teacher and ResNet8×4 student are reported.

Teacher	Student	KD	EA-KD	MLD	EA-MLD	MLD+LS	EA-MLD+LS	FCFD	EA-FCFD	Avg. Δ
64.41	55.25	56.00	59.39 +3.39	61.91	62.65 +0.74	56.45	<u>61.93</u> +5.48	60.12	60.51 +0.39	+2.50
85.07	79.62	79.64	82.40 +2.76	83.77	84.47 +0.70	81.15	<u>84.35</u> +3.20	82.90	83.22 +0.32	+1.74

Table 4. **Results on Tiny-ImageNet with Transformers.** Accuracy (%) for EA-KD and KD using transformer-based teachers and a ResNet8×4 student. Each result is averaged over three runs.

Teacher	Student	KD	EA-KD
ViT-B	71.12	ResNet8×4	54.70 57.53 +2.83
DeiT-B	85.55	55.25	56.30 58.36 +2.06
Swin-B	86.30	56.15	59.58 +3.43

Table 5. **Results on MS-COCO.** Performance of EA-KD and KD using Faster-RCNN with FPN. Metrics include AP (overall), AP₅₀, and AP₇₅.

	R-101 & R-18			R-50 & MV2		
	AP	AP ₅₀	AP ₇₅	AP	AP ₅₀	AP ₇₅
Teacher	42.04	62.48	45.88	40.22	61.02	43.81
Student	33.26	53.61	35.26	29.47	48.87	30.90
KD	33.97	54.66	36.62	30.13	50.28	31.35
EA-KD	34.78	56.14	37.19	31.81	53.18	33.18
Δ	+0.81	+1.48	+0.57	+1.68	+2.90	+1.83

Tiny-ImageNet. Tab. 3 presents results on Tiny-ImageNet across SOTA frameworks enhanced with EA. For instance, EA-KD significantly improves top-1 accuracy by 3.39% and top-5 accuracy by 2.76% over standard KD, achieving performance close to FCFD with less than a 1% difference. These results highlight EA’s effectiveness on a larger and more class-diverse dataset. Further, Tab. 4 highlights EA-KD’s ability to outperform KD when distilling from transformer-based teachers to a CNN student. While standard KD stopped improving the student when Swin-B was used as the teacher, EA-KD continued to enhance student performance, mitigating the capacity gap by allowing better teachers to produce better students.

MS-COCO. Extending to object detection, Tab. 5 presents the performance of EA-KD and KD on the MS-COCO dataset. EA-KD consistently outperforms KD across AP metrics for both model pairings, with particularly notable gains in AP₅₀. This highlights EA-KD’s ability to effectively guide the student with valuable knowledge in a more complex visual task, thereby enhancing its performance.

LLM Distillation. To explore the full potential of EA-KD, we extended our experiments to LLM distillation, applying the reweighting at the sequence level of the model outputs. As shown in Tab. 6, EA-KD consistently outperforms standard KD across datasets. Moreover, EA-KD also surpasses two recently emerging methods in this field, Re-

Table 6. **LLM Distillation Results.** Rouge-L [17] scores averaged over five seeds for KD, EA-KD, RKLD, and JSD on each dataset. SFT denotes a student fine-tuned on the dataset.

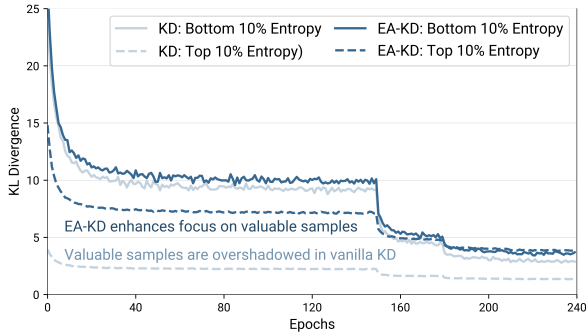
Method	Dataset					Avg.
	Dolly	SInst	Vicuna	S-NI	UnNI	
Teacher						
GPT2-XL	27.19	14.64	16.30	27.55	31.42	23.42
SFT						
GPT2-S	22.94	10.11	15.17	16.21	18.68	16.62
KD	<u>24.54</u>	10.43	15.66	17.24	20.28	17.63
RKLD	24.38	10.73	<u>15.71</u>	<u>17.31</u>	<u>20.96</u>	<u>17.82</u>
JSD	23.86	10.20	15.50	16.20	19.17	16.98
EA-KD	24.95	<u>10.59</u>	16.41	18.27	21.46	18.34
Δ to KD	+0.41	+0.16	+0.75	+1.03	+1.18	+0.71

verse KLD (RKLD) and Jensen-Shannon divergence (JSD), which aim to address KLD’s limitation of forcing the student to cover all modes of the complex LLM teacher distribution [7]. In this scenario, EA-KD’s dynamic prioritization of the most critical knowledge performed effectively in such complexity. This highlights EA-KD’s versatility beyond visual tasks, showcasing its ability to target valuable knowledge across diverse domains.

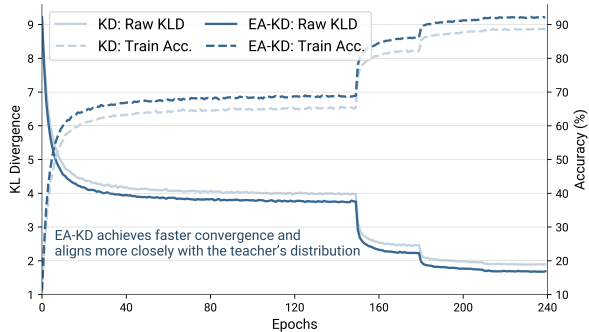
4.3. Empirical Analysis

In this section, we conduct ablation studies to evaluate two key components of EA-KD: T' and the reweighting factor. We then compare EA-KD and vanilla KD from multiple perspectives, showing how EA-KD improves teacher-student alignment and class separability. Additionally, we discuss the synergy between EA and DKD, demonstrating enhanced robustness in both the loss surface and hyperparameter stability. Finally, we highlight EA-methods computational efficiency across diverse KD frameworks.

Ablation Study. Two experiment were performed to evaluate the sensitivity of T' and the effect of each reweighting components in w_{EA} . (i) Tab. 7 shows that a T' of 3 consistently delivers optimal performance across model combinations, highlighting its robustness in reflecting sample value during distillation. (ii) As shown in Tab. 8, the single-sided factor w_{base} notably boosts baseline performance by emphasizing valuable samples, while $w_{interact}$ integrates teacher-student dynamics but may overly rely on the student responses, leading to limited gains. By combining these strengths, w_{EA} achieves superior improvement by prioritizing valuable samples and adapting to the student’s learning dynamics, enabling a precise and tailored focus.



(a) KLD for Top and Bottom 10% Entropy Samples



(b) Raw KLD and Training Accuracy (%)

Figure 5. **Comparison of KD and EA-KD During Training.** EA-KD enhances focus on high entropy samples, leading to a more effective and efficient learning process, as reflected in the overall raw KLD and training accuracy.

Table 7. **Impact of T' .** Setting T' to 3 yields the best results across architectures, demonstrating its robustness and consistency.

Teacher	Student	T'		
		2	3	4
ResNet32×4	ResNet8×4	73.90	75.46	<u>75.22</u>
WRN-28-4	WRN-16-2	74.89	75.79	<u>75.62</u>
ResNet32×4	SN-V2	75.51	75.91	<u>75.72</u>

Table 8. **Impact of Reweighting Factors.** The proposed w_{EA} outperforms the single-sided w_{base} , while $w_{interact}$, lacking teacher base guidance, shows limited improvement.

Method	Acc.	Reweighting Factor		
		w_{base}	$w_{interact}$	w_{EA}
KD [9]	73.33	<u>75.14</u> ↑	74.76 ↑	75.27 ↑
MLD [11]	77.08	<u>77.47</u> ↑	77.45 ↑	77.65 ↑
MLD+LS [30]	78.28	<u>78.30</u> ↑	78.20 ↓	78.38 ↑
FCFD [19]	76.62	<u>77.37</u> ↑	<u>77.42</u> ↑	77.44 ↑

Refined Knowledge Focus and Alignment. Fig. 5a illustrates the KLD for the top and bottom 10% entropy samples throughout training for both KD and EA-KD, with Fig. 5b depicting the overall raw KLD and training accuracy. Notably, vanilla KD’s uniform distillation causes low-entropy samples to dominate the distillation loss, failing to transfer the more critical knowledge from higher-entropy samples, as discussed in Sec. 3. Fig. 2a further illustrates this, where KD shows increasingly larger accuracy gaps with the teacher on higher entropy samples. In contrast, EA-KD refined the student’s focus on high-entropy samples and efficiently reduced the raw KLD (Fig. 5), achieving improved mimicry and generalization with more consistent alignment to the teacher across entropy segments (Fig. 2a).

Student’s Unique Perspective. Fig. 6 compares the t-SNE visualizations [33] of KD and EA-KD with the high H^S and w_{EA} samples highlighted. Similar to Fig. 2b, high H^S samples also lie near decision boundaries in the KD-student. This suggests that, despite having a different view

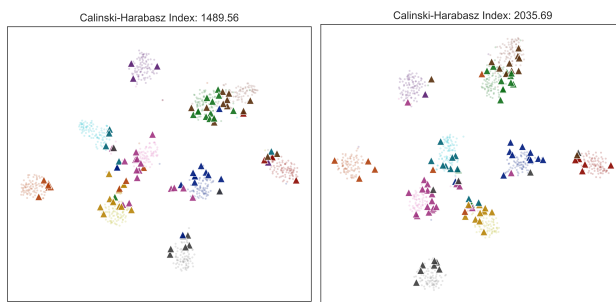


Figure 6. **t-SNE of Students.** Top 10% high H^S samples for KD (left) and w_{EA} samples for EA-KD (right) are highlighted with triangles. High H^S samples cluster near decision boundaries, underscoring their learning value for the student. EA-KD achieves better class separability as indicated by a higher CH index.

from the teacher (Fig. 3), the student’s evolving capacity enables H^S to capture the samples crucial for its own learning progress³. In EA-KD, integrating both H^T and H^S in w_{EA} allows us to harness the complementary strengths of the teacher’s informed assessment and the student’s dynamic learning needs. Consequently, EA-KD achieves superior class separability as indicated by a higher Calinski-Harabasz (CH) index.

Consistency in Entropy Levels. As shown in Fig. 3, EA-KD mitigates the increasing entropy variation across epochs observed in KD, enabling the student to maintain more stable H^S and align more closely to H^T . This stability creates a feedback loop in EA-KD, where a steady H^S leads to a stable w_{EA} , promoting a more focused learning process. As a result, the student more effectively mimics the teacher’s response and achieves improved performance.

Loss Landscape and Synergy in EA-DKD. Visualizing the loss landscape [15] offers insights into the student’s robustness against noise and generalization. As illustrated in Fig. 7, DKD shows narrow and fluctuating contours with

³See Appendix A.1 for further t-SNE visualizations showing the student’s evolving sample focus over training epochs.

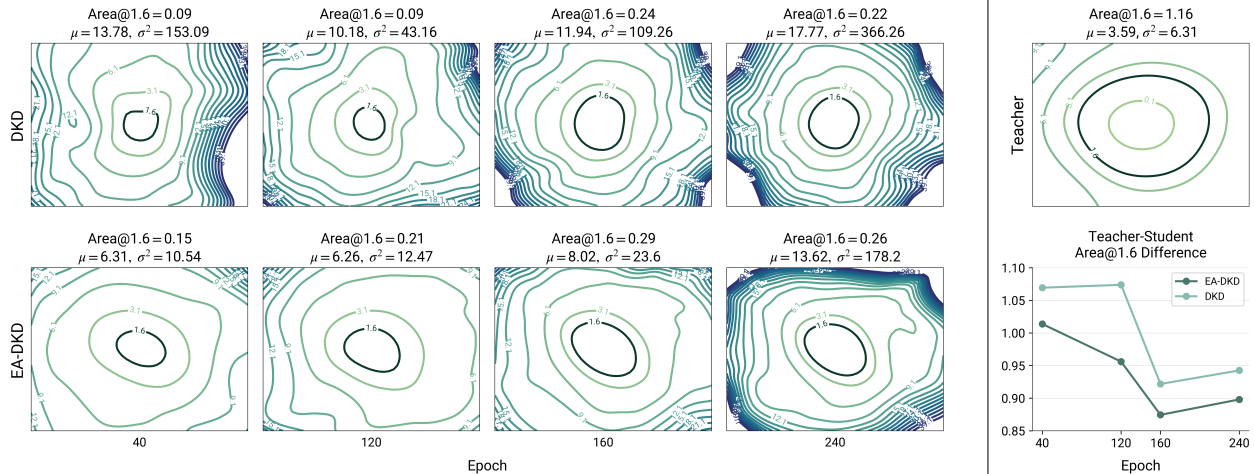


Figure 7. **Loss Surface and Differences in Area@1.6 for DKD and EA-DKD Students Across Epochs.** The mean and variance for the surface, along with the contour areas at level 1.6 (Area@1.6), are provided for each subplot. The line plot (lower right) tracks the differences in Area@1.6 between the teacher and students over epochs. EA-DKD consistently shows larger contours with less fluctuation, signifying smoother learning surfaces and a more robust generalization process compared to DKD.

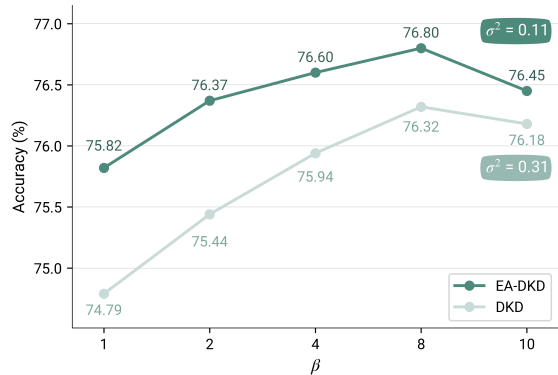


Figure 8. **Comparison of DKD and EA-DKD Performance Across Varying β Values.** EA-DKD consistently outperforms DKD and significantly reduces performance variance over β (0.10 vs. 0.31), highlighting EA-DKD’s enhanced robustness.

significantly higher variance across epochs (e.g. 366.26 at epoch 240), indicating instability in the loss surface and weaker generalization. In contrast, EA-DKD consistently produces a smoother surface with more stable contours (e.g. variance of 178.20 at epoch 240) and broader low-loss regions (Area@1.6) compared to DKD, suggesting improved generalizability. In addition, the Area@1.6 comparison (Fig. 7, lower right) underscores EA-DKD’s closer alignment with the teacher’s surface throughout training.

The enhanced generalization in EA-DKD also extends to the robustness of its hyperparameter. DKD was introduced to decouple target class KD (TCKD) and non-target class KD (NCKD) in vanilla KD, balancing them with hyperparameters α and β [38]. While α remains stable around 1.0, adjusting β from 1.0 to 10.0 leads to fluctuating performance [38], with a variance of 0.31 (see Fig. 8). Notably, EA-DKD effectively reduces this fluctuation to a variance

of 0.10 and consistently improves the performance. Overall, the enhanced generalizability and robustness may be attributed to the synergy between DKD and EA in handling different aspects of knowledge transfer: DKD prevents NCKD from being overshadowed by TCKD at the class level, while EA ensures valuable samples—often rich in NCKD—are not dominated by simpler ones at the sample level. Additionally, the dynamic focus in EA compensates for the static nature of β . Together, EA-DKD facilitates a more balanced and efficient knowledge transfer process, both class-wise and sample-wise.

Computational Efficiency. Fig. 1 illustrates the efficiency of EA-methods, showing significant performance improvements on various SOTA KD frameworks with negligible cost. This remarkable computational efficiency, combined with its streamlined integration into both logit- and feature-based KD frameworks, suggests the potential of our method as a versatile and accessible enhancement for KD.

5. Conclusion

In this paper, we examined existing KD methods from a novel perspective, revealing the limitation of their inherent uniform distillation scheme, which often hinders the transfer of valuable, high-entropy samples that contain critical knowledge. To overcome this, we introduced EA-KD, a plug-and-play KD approach that dynamically reweights the distillation loss, directing the learning process toward valuable samples. EA-KD consistently improves SOTA KD methods across image classification, object detection, and LLM distillation, all with negligible cost. We believe EA-KD showcases a great paradigm of the meticulous handling of knowledge transfer, offering sample-wise adaptability while integrating the student’s evolving learning dynamics into the distillation process.

References

- [1] Pengguang Chen, Shu Liu, Hengshuang Zhao, and Jiaya Jia. Distilling knowledge via knowledge review. In *Proceedings of the IEEE/CVF Conference on Computer Vision and Pattern Recognition*, pages 5008–5017, 2021. 1, 3, 5
- [2] Xu Cheng, Zhefan Rao, Yilan Chen, and Quanshi Zhang. Explaining knowledge distillation by quantifying the knowledge. *CoRR*, abs/2003.03622, 2020. 3
- [3] Wei-Lin Chiang, Zhuohan Li, Zi Lin, Ying Sheng, Zhanghao Wu, Hao Zhang, Lianmin Zheng, Siyuan Zhuang, Yonghao Zhuang, Joseph E. Gonzalez, Ion Stoica, and Eric P. Xing. Vicuna: An open-source chatbot impressing gpt-4 with 90%* chatgpt quality, 2023. 5
- [4] Mike Conover, Matt Hayes, Ankit Mathur, Jianwei Xie, Jun Wan, Sam Shah, Ali Ghodsi, Patrick Wendell, Matei Zaharia, and Reynold Xin. Free dolly: Introducing the world’s first truly open instruction-tuned llm, 2023. 5
- [5] Jacob Devlin, Ming-Wei Chang, Kenton Lee, and Kristina Toutanova. BERT: Pre-training of deep bidirectional transformers for language understanding. In *Proceedings of the 2019 Conference of the North American Chapter of the Association for Computational Linguistics: Human Language Technologies, Volume 1 (Long and Short Papers)*, pages 4171–4186, Minneapolis, Minnesota, 2019. Association for Computational Linguistics. 1
- [6] Alexey Dosovitskiy, Lucas Beyer, Alexander Kolesnikov, Dirk Weissenborn, Xiaohua Zhai, Thomas Unterthiner, Mostafa Dehghani, Matthias Minderer, Georg Heigold, Sylvain Gelly, Jakob Uszkoreit, and Neil Houlsby. An image is worth 16x16 words: Transformers for image recognition at scale. In *International Conference on Learning Representations*, 2021. 1, 5
- [7] Yuxian Gu, Li Dong, Furu Wei, and Minlie Huang. Minillm: Knowledge distillation of large language models. In *The Twelfth International Conference on Learning Representations*, 2024. 5, 6
- [8] Kaiming He, Xiangyu Zhang, Shaoqing Ren, and Jian Sun. Deep residual learning for image recognition. In *Proceedings of the IEEE conference on computer vision and pattern recognition*, pages 770–778, 2016. 5
- [9] Geoffrey Hinton, Oriol Vinyals, and Jeff Dean. Distilling the knowledge in a neural network. *arXiv preprint arXiv:1503.02531*, 2015. 1, 2, 3, 5, 7
- [10] Or Honovich, Thomas Scialom, Omer Levy, and Timo Schick. Unnatural instructions: Tuning language models with (almost) no human labor. *arXiv preprint arXiv:2212.09689*, 2022. 5
- [11] Ying Jin, Jiaqi Wang, and Dahua Lin. Multi-level logit distillation. In *Proceedings of the IEEE/CVF Conference on Computer Vision and Pattern Recognition*, pages 24276–24285, 2023. 1, 3, 5, 7
- [12] Alex Krizhevsky. Learning multiple layers of features from tiny images. Technical report, University of Toronto, 2009. 5
- [13] Kisoo Kwon, Hwidong Na, Hoshik Lee, and Nam Soo Kim. Adaptive knowledge distillation based on entropy. In *ICASSP 2020 - 2020 IEEE International Conference on Acoustics, Speech and Signal Processing (ICASSP)*, pages 7409–7413, 2020. 1, 3
- [14] Ya Le and Xuan Yang. Tiny imagenet visual recognition challenge. *CS 231N*, 7(7):3, 2015. 5
- [15] Hao Li, Zheng Xu, Gavin Taylor, Christoph Studer, and Tom Goldstein. Visualizing the loss landscape of neural nets. In *Neural Information Processing Systems*, 2018. 7
- [16] Zheng Li, Xiang Li, Lingfeng Yang, Borui Zhao, Renjie Song, Lei Luo, Jun Li, and Jian Yang. Curriculum temperature for knowledge distillation. In *Proceedings of the AAAI Conference on Artificial Intelligence*, pages 1504–1512, 2023. 1, 3, 5
- [17] Chin-Yew Lin. Rouge: A package for automatic evaluation of summaries. In *Text summarization branches out*, pages 74–81, 2004. 6
- [18] Tsung-Yi Lin, Michael Maire, Serge Belongie, James Hays, Pietro Perona, Deva Ramanan, Piotr Dollár, and C Lawrence Zitnick. Microsoft coco: Common objects in context. In *Computer Vision—ECCV 2014: 13th European Conference, Zurich, Switzerland, September 6–12, 2014, Proceedings, Part V 13*, pages 740–755. Springer, 2014. 5
- [19] Dongyang Liu, Meina Kan, Shiguang Shan, and CHEN Xilin. Function-consistent feature distillation. In *The Eleventh International Conference on Learning Representations*, 2022. 1, 3, 5, 7
- [20] Jihao Liu, Boxiao Liu, Hongsheng Li, and Yu Liu. Meta knowledge distillation. *arXiv preprint arXiv:2202.07940*, 2022. 3
- [21] Ze Liu, Yutong Lin, Yue Cao, Han Hu, Yixuan Wei, Zheng Zhang, Stephen Lin, and Baining Guo. Swin transformer: Hierarchical vision transformer using shifted windows. In *Proceedings of the IEEE/CVF international conference on computer vision*, pages 10012–10022, 2021. 1, 5
- [22] Peng Lu, Abbas Ghaddar, Ahmad Rashid, Mehdi Rezagholizadeh, Ali Ghodsi, and Philippe Langlais. RW-KD: Sample-wise loss terms re-weighting for knowledge distillation. In *Findings of the Association for Computational Linguistics: EMNLP 2021*, pages 3145–3152, Punta Cana, Dominican Republic, 2021. Association for Computational Linguistics. 3
- [23] Ningning Ma, Xiangyu Zhang, Hai-Tao Zheng, and Jian Sun. Shufflenet v2: Practical guidelines for efficient cnn architecture design. In *Proceedings of the European conference on computer vision (ECCV)*, pages 116–131, 2018. 5
- [24] Seyed Iman Mirzadeh, Mehrdad Farajtabar, Ang Li, Nir Levine, Akihiro Matsukawa, and Hassan Ghasemzadeh. Improved knowledge distillation via teacher assistant. In *Proceedings of the AAAI conference on artificial intelligence*, pages 5191–5198, 2020. 1
- [25] Alec Radford, Jeff Wu, Rewon Child, David Luan, Dario Amodei, and Ilya Sutskever. Language models are unsupervised multitask learners. *OpenAI blog*, 2019. 1, 5
- [26] Adriana Romero, Nicolas Ballas, Samira Ebrahimi Kahou, Antoine Chassang, Carlo Gatta, and Yoshua Bengio. Fitnets: Hints for thin deep nets. *arXiv preprint arXiv:1412.6550*, 2014. 1, 3
- [27] Mark Sandler, Andrew Howard, Menglong Zhu, Andrey Zhmoginov, and Liang-Chieh Chen. Mobilenetv2: Inverted

- residuals and linear bottlenecks. In *Proceedings of the IEEE conference on computer vision and pattern recognition*, pages 4510–4520, 2018. 5
- [28] Claude Elwood Shannon. A mathematical theory of communication. *The Bell system technical journal*, 27(3):379–423, 1948. 1, 3
- [29] K Simonyan and A Zisserman. Very deep convolutional networks for large-scale image recognition. In *3rd International Conference on Learning Representations (ICLR 2015)*. Computational and Biological Learning Society, 2015. 5
- [30] Shangquan Sun, Wenqi Ren, Jingzhi Li, Rui Wang, and Xiaochun Cao. Logit standardization in knowledge distillation. In *Proceedings of the IEEE/CVF Conference on Computer Vision and Pattern Recognition*, pages 15731–15740, 2024. 3, 5, 7
- [31] Yonglong Tian, Dilip Krishnan, and Phillip Isola. Contrastive representation distillation. *arXiv preprint arXiv:1910.10699*, 2019. 5
- [32] Hugo Touvron, Matthieu Cord, Matthijs Douze, Francisco Massa, Alexandre Sablayrolles, and Hervé Jégou. Training data-efficient image transformers & distillation through attention. In *International conference on machine learning*, pages 10347–10357. PMLR, 2021. 1, 5
- [33] Laurens Van der Maaten and Geoffrey Hinton. Visualizing data using t-sne. *Journal of machine learning research*, 9 (11), 2008. 2, 7
- [34] Yizhong Wang, Yeganeh Kordi, Swaroop Mishra, Alisa Liu, Noah A Smith, Daniel Khashabi, and Hannaneh Hajishirzi. Self-instruct: Aligning language models with self-generated instructions. *arXiv preprint arXiv:2212.10560*, 2022. 5
- [35] Yizhong Wang, Swaroop Mishra, Pegah Alipoormolabashi, Yeganeh Kordi, Amirreza Mirzaei, Anjana Arunkumar, Arjun Ashok, Arut Selvan Dhanasekaran, Atharva Naik, David Stap, et al. Super-naturalinstructions: Generalization via declarative instructions on 1600+ nlp tasks. *arXiv preprint arXiv:2204.07705*, 2022. 5
- [36] Sergey Zagoruyko and Nikos Komodakis. Wide residual networks. In *Proceedings of the British Machine Vision Conference 2016*. British Machine Vision Association, 2016. 5
- [37] Songming Zhang, Xue Zhang, Zengkui Sun, Yufeng Chen, and Jinan Xu. Dual-space knowledge distillation for large language models. *arXiv preprint arXiv:2406.17328*, 2024. 5
- [38] Borui Zhao, Quan Cui, Renjie Song, Yiyu Qiu, and Jiajun Liang. Decoupled knowledge distillation. In *Proceedings of the IEEE/CVF Conference on computer vision and pattern recognition*, pages 11953–11962, 2022. 1, 3, 5, 8

EA-KD: Entropy-based Adaptive Knowledge Distillation

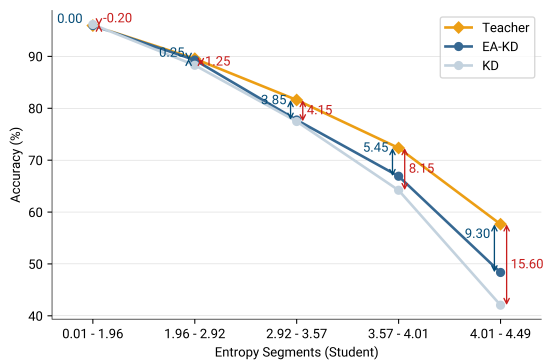
Supplementary Material

A. Additional Analysis and Visualizations

This document provides additional analysis to complement the main paper. It includes a detailed examination of high student entropy samples, loss landscape comparisons for KD and EA-KD, and t-SNE visualizations for various KD frameworks and their EA-enhanced variants.

A.1. Analysis of High Student Entropy Samples

Complementary to the teacher entropy analysis in Sec. 1, this section emphasizes the critical role of high student entropy samples in the adaptive reweighting process of EA-KD. As shown in Fig. A1a, high student entropy samples correlate with larger teacher-student accuracy gaps similar to the teacher entropy segments (Fig. 2a). Additionally, Fig. A1b presents the students’ t-SNE visualizations across training epochs for KD and EA-KD, with high-entropy samples (H^S) and reweighted samples (w_{EA}) highlighted, respectively. Notably, these high-entropy samples also cluster near decision boundaries similar to the teacher’s t-SNE (Fig. 2b). Unlike the teacher, however, the student’s top-entropy samples shift dynamically over training. For instance, in KD, the yellow class at epoch 40 is located near the center of most clusters and contains numerous high-entropy samples. By epoch 120, high-entropy samples are more prevalent in the green and purple classes as they shift closer to the center. With this dynamic integrated into w_{EA} , EA-KD continuously adapts to the student’s evolving learning needs throughout training, complementing the static nature of w_{base} and fostering a tailored knowledge transfer.



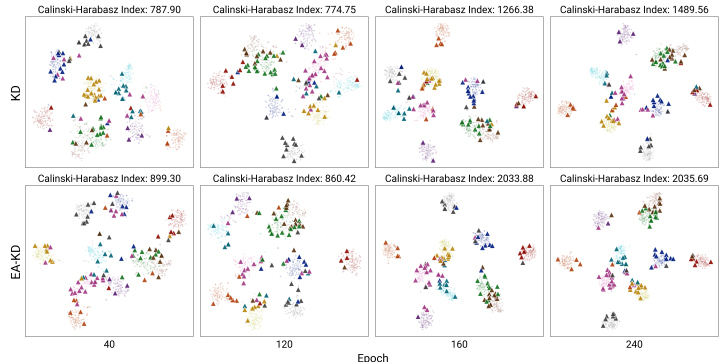
(a) Accuracy vs. Student Entropy Segments.

A.2. Loss Landscape Analysis for KD and EA-KD

We further analyze the robustness of KD and EA-KD by examining their loss landscapes across training epochs. As shown in Fig. A2, EA-KD achieves a consistently smoother loss surface compared to KD (*e.g.* σ^2 of 217.68 vs. 305.21 at epoch 240) and larger Area@1.6 values. Notably, KD’s Area@1.6 metric remains 0 at epochs 40 and 120, indicating the absence of low-loss regions. In contrast, EA-KD achieves values of 0.01 and 0.05, respectively, underscoring its improved learning efficiency by enabling the student to assimilate the key knowledge. These results highlight EA-KD’s ability to ensure a more efficient and effective optimization, facilitating enhanced generalizability compared to standard KD.

A.3. t-SNE of KD Frameworks and EA-methods

The t-SNE visualizations of students from various KD frameworks and their EA-method variants, alongside the teacher’s representation, are shown in Fig. A3. EA-methods consistently exhibit more distinct and well-defined class clusters compared to their respective baselines, as evidenced by higher CH indices. Remarkably, the SOTA EA-MLD+LS achieves the highest CH index of 814.96, indicating its superior performance and closer alignment with the teacher. Furthermore, although EA-DKD ranks fourth in performance (Tab. 2), it demonstrates the second-best class separability, underscoring its enhanced robustness as discussed in Sec. 4.3. These findings highlight EA-KD’s versatility in enhancing class separability and improving knowledge transfer across diverse KD frameworks.



(b) t-SNE of Students Across Training Epochs.

Figure A1. **High Student Entropy Analysis in KD and EA-KD.** (a) Higher student entropy samples correlate with larger accuracy gaps in KD. EA-KD demonstrates closer alignment with the teacher, particularly in high-entropy regions. (b) High H^S samples consistently cluster near decision boundaries, reflecting the student’s real-time learning needs. EA-KD adapts to this dynamic, achieving enhanced class separability over epochs.

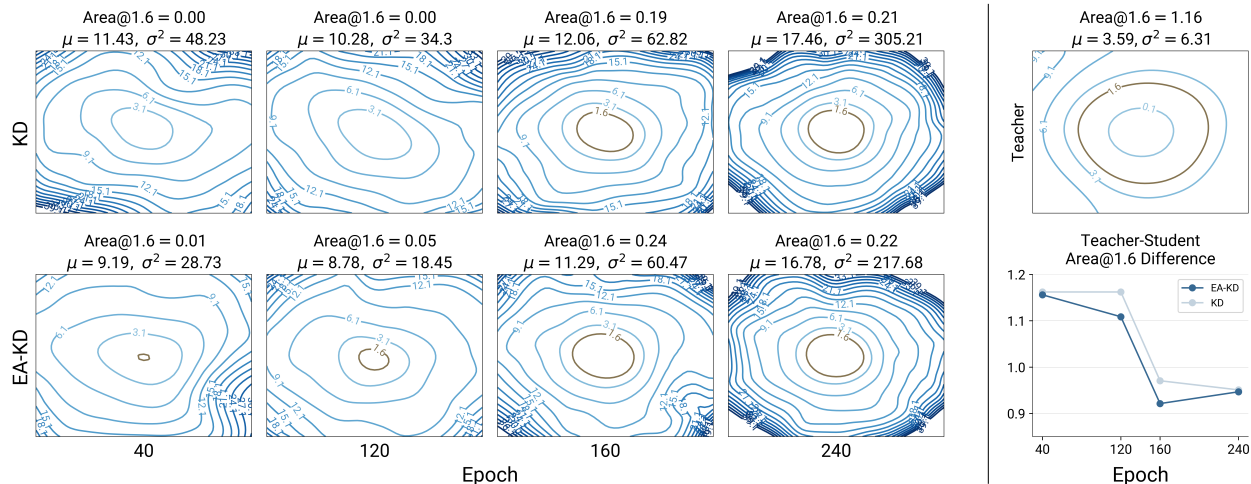


Figure A2. **Loss Surface and Differences in Area@1.6 for KD and EA-KD Students Across Epochs.** Contour plots illustrate the loss landscapes of KD (first row) and EA-KD (second row) across training epochs. The line plot (lower right) tracks the differences in Area@1.6 between the teacher and students over epochs. EA-KD exhibits a more stable and robust loss surface, with greater Area@1.6 earlier in training, signifying a more efficient learning process.



Figure A3. **t-SNE Visualizations of EA-methods vs. Baselines.** The students from various KD frameworks (first and third row) and their EA-enhanced counterparts (second and fourth row), along with the teacher (lower right), are shown. EA-methods consistently achieve higher CH indices, indicating better class separability.